

Analyses of Near- and Far-Field Two-Lobe Patterns Outside the Output Endface of a Two-Mode Fiber

A WANG, G Z WANG, and R O CLAUS

Fiber & Electro-Optics Research Center, Bradley Department of Electrical Engineering,
Virginia Polytechnic Institute and State University, Blacksburg, VA 24061-0111

ABSTRACT: The behaviors of the near- and far-field two-lobe radiation patterns from a circular-core two-mode fiber are studied by using both the mode and Kirchhoff diffraction theories. The electric field outside the output endface of the fiber is derived from the electric field distribution of the LP_{01} and LP_{11} modes at the fiber endface using the Kirchhoff diffraction formula. Different phenomena are studied by solving this expression numerically at near- and far-fields. The Gouy phase shifts are quantitatively evaluated at cross-sections of the near field. The results reveal the distortion and dislocation of the far-field two-lobe pattern induced by an inclination angle of the fiber endface.

1. INTRODUCTION

Recently there has been considerable interest in various circular-core and elliptical-core (e-core) two-mode fiber optic components and devices. Different components and devices such as intermodal couplers, modal filters, acoustic-optic frequency shifters and fiber sensors were demonstrated by Blake et al (1986), Kim et al (1987), Kim et al (1986) and Murphy et al (1990), respectively. A detailed evaluation of external perturbation on the differential phase shifts between the two modes was presented by Huang et al (1990) for an e-core two-mode fiber. The Gouy phase shift of the two-lobe pattern at the output of the e-core two-mode fiber was also reported by Huang et al (1989) in their discussion of a strain sensing application. The dependence of the differential propagation constant between the two modes on the ellipticity of the fiber core and on other parameters was studied by Shaw et al (1990). To date, some work have been done to analyze light propagation characteristics in two-mode fiber and their dependence upon various physical parameters, such as core ellipticity and wavelength. However, in developing and designing most two-mode fiber devices, the knowledge of the near- and far-field two-lobe patterns owing to the interference between the LP_{01} and even LP_{11} modes is required. Although some far-field two-lobe patterns have been studied experimentally, detailed information of the behavior of the two-lobe pattern at the near and far-field, as well as their relationship, is essential for a thorough understanding of such effects and for the optimum design of two-mode fiber-optic devices.

In this paper we describe the propagation characteristics of the two-lobe radiation pattern from the output endface of the fiber to the far-field employing Kirchhoff diffraction theory.

2. THEORY

Weakly-guiding circular-core single-mode fibers support two orthogonal polarization modes (HE_{11}^x and HE_{11}^y), designated LP_{01} . They are the fundamental modes and have the same spatial

intensity distribution. The next four higher order modes are TE_{01} , TM_{01} , even HE_{21} and odd HE_{21} . In the weakly guiding approximation, these four modes have almost the same propagation constants and the same cross-sectional intensity distributions, and are denoted as the LP_{11} mode. Fibers operating in the LP_{01} and LP_{11} regime are called two-mode optical fibers. For an elliptical core two-mode fiber, because of the asymmetry of the fiber core, the degeneracy of LP_{11} is broken into even LP_{11} and odd LP_{11} modes. Hence only the LP_{01} and even LP_{11} modes can be guided in an e-core fiber. In the analysis below, we assume the LP_{01} and even LP_{11} modes are excited in a circular-core fiber and no coupling between the even LP_{11} and odd LP_{11} modes takes place.

For a weakly-guiding circular-core fiber, the electrical field amplitudes of the LP_{01} and even LP_{11} modes can be expressed as (Safaai-Jazi et al 1988)

$$\Psi_{01} = A_{01} J_0(\kappa_{01} \rho) \exp(j\beta_{01} z) \exp(-j\omega t), \quad (2a)$$

and

$$\Psi_{11} = A_{11} J_1(\kappa_{11} \rho) \cos(\phi) \exp(j\beta_{11} z) \exp(-j\omega t), \quad (2b)$$

where $\kappa_{lm}^2 = \omega^2 n_1^2 / c^2 - \beta_{lm}^2$, ω is the angular frequency, and β_{lm} is the longitudinal propagation constant of the mode. A_{lm} is the amplitude coefficient of the mode. ρ and ϕ , correspond to the radial and angular coordinates, respectively. We assume the electric fields of these two modes at the output endface of the fiber core region can also be approximately given by Eqs. (2a) and (2b), respectively. Then, the total electric field at the endface of fiber core can be written as

$$\Psi_T = \Gamma J_0(\kappa_{01} \rho) \exp(j\beta_{01} z) + J_1(\kappa_{11} \rho) \cos(\phi) \exp(j\beta_{11} z), \quad (3)$$

where Γ is the normalized amplitude coefficient and z represents the length of the fiber. Note that we have omitted the term of $\exp(j\omega t)$ in Eq. (3).

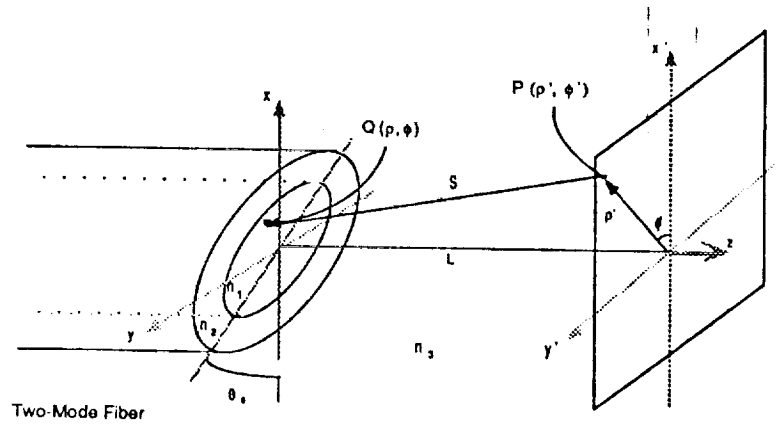


Figure 1. Coordinate system for the calculation.

The coordinate configuration used to evaluate the electric field outside the fiber endface is shown in Figure 1. The electric field at a point P outside the e-core two-mode fiber endface is given by the

Kirchhoff diffraction formula as (Born and Wolf 1975)

$$\psi(P) = \frac{-1}{4\pi} \iint \left[\psi_T \frac{\partial}{\partial z} \left(\frac{\exp(jkS)}{S} \right) - \frac{\exp(jkS)}{S} \frac{\partial \psi_T}{\partial z} \right] ds, \quad (5)$$

where k is the free space propagation constant and S is the distance between P and Q . The integral is evaluated over the entire core region of the two-mode fiber. Without scarifying any significant accuracy, we ignored the contributions due to the fields in the cladding region. In general, the endface of the fiber is not perpendicular to the fiber axis. An angle θ_0 is introduced to represent the inclination of the endface with respect to the x axis as shown in Figure 1. From geometry, S can be expressed as

$$S = (\rho'^2 + \rho^2 - 2\rho\rho'\cos(\phi - \phi') + (z' - z_0 - \rho \cos \phi \tan \theta_0)^2)^{1/2}. \quad (6)$$

Substituting Eqs. (3) and (6) into Eq. (5), we can evaluate the electrical field at point P . Defining $C(P)$ and $D(P)$ to be the real and imaginary parts of $\psi(P)$, respectively, we can write a compact expression for the intensity at the point P as

$$I(P) = [C(P)]^2 + [D(P)]^2, \quad (7)$$

where $C(P)$ is given by

$$\begin{aligned} C(P) = \frac{-1}{4\pi} \iint \frac{1}{S} \left\{ \left(-\Gamma J_0(\kappa_{01}\rho) \sin \phi_1 - J_1(\kappa_{11}\rho) \cos \phi \sin \phi_2 \right) k \frac{\partial S}{\partial n} \right. \\ \left. - \left(\frac{1}{S} \frac{\partial S}{\partial n} \right) \left(\Gamma J_0(\kappa_{01}\rho) \cos \phi_1 + J_1(\kappa_{11}\rho) \cos \phi \cos \phi_2 \right) \right. \\ \left. + \Gamma k A_\phi J_0(\kappa_{01}\rho) \sin \phi_1 - \Gamma \kappa_{01} J_1(\kappa_{01}\rho) \cos \phi_1 \cos \phi \sin \theta_0 \right. \\ \left. + k A_\phi \cos \phi J_1(\kappa_{11}\rho) \sin \phi_2 \right. \\ \left. + \left(\frac{\kappa_{11}}{2} \cos \phi_2 \sin \theta_0 \right) \left(J_0(\kappa_{01}\rho) - J_2(\kappa_{11}\rho) \cos 2\phi \right) \right\} ds, \end{aligned} \quad (8)$$

and $D(P)$ is expressed as

$$\begin{aligned} D(P) = \frac{-1}{4\pi} \iint \frac{1}{S} \left\{ \left(\Gamma J_0(\kappa_{01}\rho) \cos \phi_1 + J_1(\kappa_{11}\rho) \cos \phi \cos \phi_2 \right) k \frac{\partial S}{\partial n} \right. \\ \left. - \left(\frac{1}{S} \frac{\partial S}{\partial n} \right) \left(\Gamma J_0(\kappa_{01}\rho) \cos \phi_1 + J_1(\kappa_{11}\rho) \cos \phi \sin \phi_2 \right) \right. \\ \left. - \Gamma k A_\phi J_0(\kappa_{01}\rho) \cos \phi_1 + \Gamma \kappa_{01} J_1(\kappa_{01}\rho) \sin \phi_1 \cos \phi \sin \theta_0 \right. \\ \left. + k A_\phi \cos \phi J_1(\kappa_{11}\rho) \cos \phi_2 \right. \\ \left. + \left(\frac{\kappa_{11}}{2} \cos \phi_2 \sin \theta_0 \right) \left(J_0(\kappa_{01}\rho) - J_2(\kappa_{11}\rho) \cos 2\phi \right) \right\} ds, \end{aligned} \quad (9)$$

where $A_\phi = 2 \cos \phi - \csc \phi$, $\phi_1 = \beta_{01} z + k S$ and $\phi_2 = \beta_{11} z + k S$. Note that since electromagnetic waves propagate in the free space outside the fiber endface, in the above calculation, $\partial/\partial z(\exp(j\beta_{1m}z))$ is replaced by $j\beta_{1m} \exp(j\beta_{1m}z)$. By numerically solving Eqs. (8) and (9) and substituting the calculated results into Eq. (7), we can obtain an optical intensity at any point in space outside the fiber endface. By evaluating the intensity at each point on a cross sectional area outside the fiber endface, we can map the optical intensity distribution over that cross sectional area.

3. COMPUTER SIMULATION

To numerically evaluate the diffraction expression, we set $\beta_{01} = 14.654 \text{ rad./}\mu\text{m}$, $\beta_{11} = 14.591 \text{ rad./}\mu\text{m}$, $a = 1.25 \mu\text{m}$, $n_1 = 1.489$, $\Gamma = 0.6$, and $\lambda = 633 \text{ nm}$. To obtain the normal two-lobe pattern, we choose $\theta_0 = 0$ (the edge of the fiber endface is perpendicular to the fiber axis). Figure 2 shows the numerical evaluations of Eqs. (7), (8) and (9) obtained by setting the differential phase delay $\Delta\phi$, given by $\Delta\phi = \Delta\beta z$, between the LP_{01} and even LP_{11} modes to be equal to $\Delta\phi = 0, \pi/2, \pi$ and $3\pi/2$, respectively. This demonstrates the well known two-lobe oscillation effect commonly observed in experiments. Most two-mode fiber devices and instrumentation are implemented based on this effect.

In physical optics, the Gouy effect describes the fact that a certain amount of phase shift will be introduced when a Gaussian beam travels through a focal region (Siegman 1986). For the two-mode fiber, the fiber endface can be considered equivalently as such a focus. A Gouy phase shift in the two-lobe pattern outside fiber endface is verified as indicated in Figure 3. It is noted that the maximum phase shift occurs within $20 \mu\text{m}$ from the endface. This phase variation is almost negligible when light propagates more than $200 \mu\text{m}$ from the endface.

Deformation of the far-field two-lobe pattern which corresponds to different endface inclination angles θ_0 is presented in Figures 4a and 4b. These results indicate that distortion of the two-lobe pattern is associated with the spatial dislocation of the pattern. The decrease in the total power is caused by the increase in the Fresnel reflection at the fiber endface with increasing

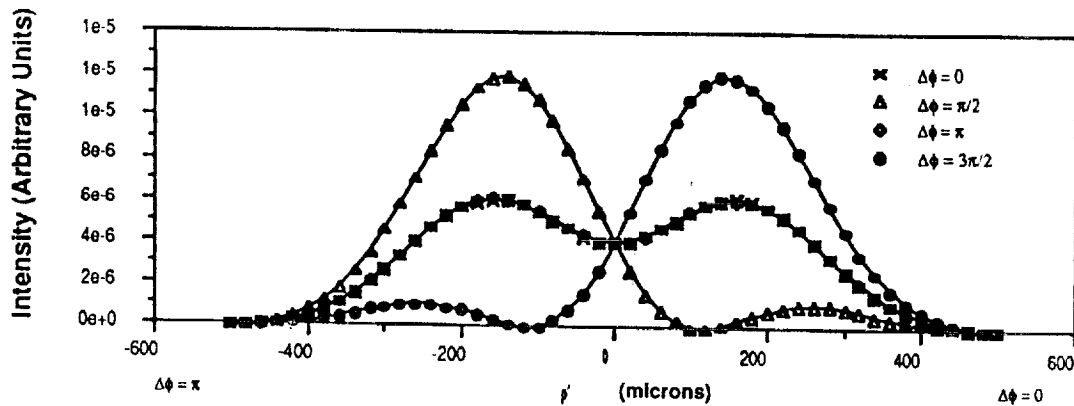


Figure 2. Far-field two-lobe patterns with different differential phase delays.

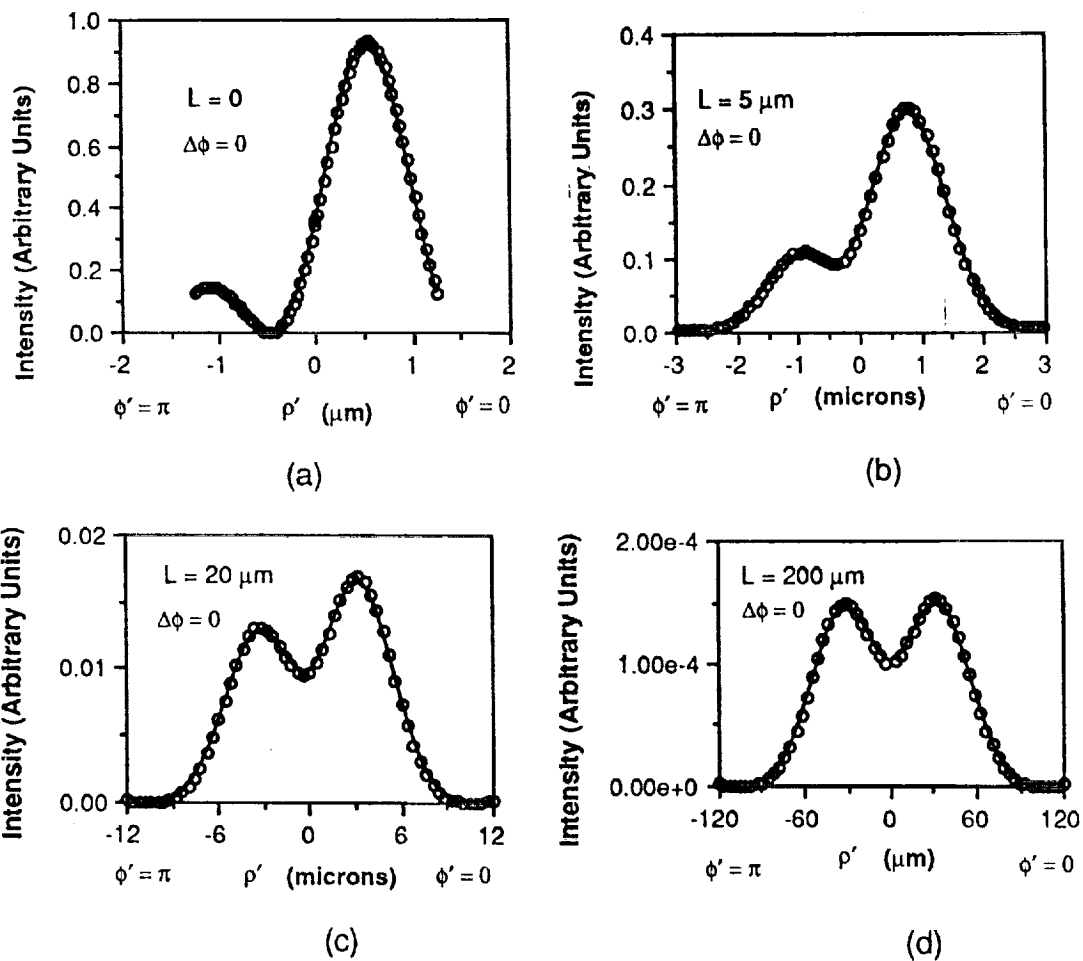


Figure 3. Two-lobe intensity pattern cross-sections at different distances from the fiber endface.

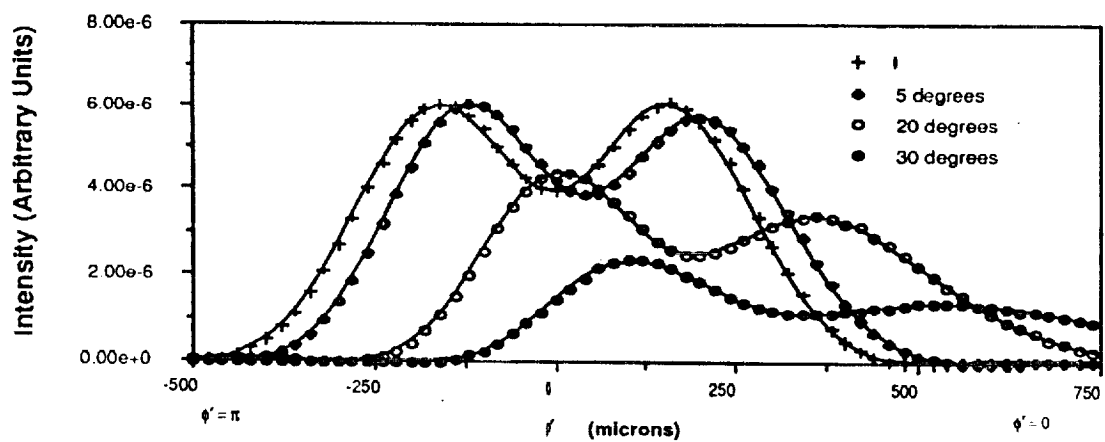


Figure 4. Far-field two-lobe patterns at $L=1\text{ mm}$ from different angles of the fiber endface.

θ_0 . This effect has been employed to fabricate a two-mode fiber sensor for simultaneous measurement of strain and temperature (Wang et al 1991). The difference in the heights of the two peaks becomes observable at $\theta_0 = 5^\circ$. This implies that the angle error of the fiber endface must be controlled within few degrees in order to obtain high quality performance in two-mode fiber devices.

CONCLUSION

A detailed analysis of the two-lobe radiation pattern outside a circular-core two-mode fiber endface is presented by using the electric field expressions of linearly polarized modes and Kirchhoff diffraction theory. The important physical phenomena observed in experiments, such as the two-lobe oscillation, the effect of the Gouy phase shift, and the deformation of the two-lobe pattern, are confirmed. This theoretical model is simple and effective. It may also serve researchers as a vehicle to solve other near- and far-field problems in developing fiber optic components.

REFERENCES

- Blake J N, Kim B Y, and Shaw H J 1986 *Opt. Lett.* **11**, pp. 177-9
- Kim B Y, Blake J N, Huang S Y, and Shaw H J 1987 *Opt. Lett.* **12** pp. 729-31
- Kim B Y, Blake J N, Engan H, and Shaw H J *Opt. Lett.* **11** pp. 389-9
- Murphy K A, Miller M S, Vengsarkar A M, and Claus R O 1990 *J. Lightwave Technology* **8** pp 1688-96
- Huang S Y, Blake J N, and Kim B Y 1990 *J. Lightwave Technology* **8**, pp 23-33
- Huang S Y, Park H J, and Kim B Y 1989 *Opt. Lett.* **14** pp 1380-2
- Shaw J K, Vengsarkar A M, Claus R O 1990 *Proc. SPIE* San Jose CA
- Safaai-Jazi A and Claus R O 1988 *Proc. SPIE-Int. Soc. Opt. Eng.* **986** p180
- Born M and Wolf E 1975 *Principles of Optics - Electromagnetic Theory of Propagation, Interference and Diffraction of Light* (Pergamon Press, sixth edition) pp. 375-82
- Siegman A E, *Lasers* (University Science Books, Mill Valley, California., 1986), Chapter 17 and references therein
- Wang A, Wang Z G, Vengsarkar A M, and Claus R O 1991 *Proc. SPIE: Laser and Optical Fiber Sensors* (Boston) pp 294-303